Ligand-induced conformation change in folate-binding protein

Niels C. KAARSHOLM,*§ Anne-Marie KOLSTRUP,* Susan E. DANIELSEN,* Jan HOLM† and Steen I. HANSEN‡

*Novo Research Institute, Novo Nordisk A/S, DK-2880 Bagsvaerd, Denmark, and Departments of Clinical Chemistry, Central Hospitals of †Nykøbing Falster, DK-4800 and ‡Hillerød, DK-3400, Denmark

C.d. and fluorescence spectroscopy have been used to investigate the effect of ligand binding on the structure and stability of folate-binding protein (FBP) from cow's whey. The c.d. spectrum of unligated FBP predicts the following secondary structure: 22% helix, 25% antiparallel β-strand, 5% parallel β-strand, 17% turn and 31% random-coil structure. Folate binding to FBP results in significant changes in the c.d. spectrum. Analysis of the spectrum shows a 10% decrease in antiparallel β-strand as a result of ligand binding. Folate binding also leads to strong quenching of FBP tryptophan fluorescence. The magnitude of the quench is proportional to ligand binding. The guanidinium chloride-induced unfolding of FBP is shown to be a multistate process. Detection by c.d. and fluorescence spectroscopy lead to non-identical transitions. Modelling studies are consistent with the existence of a stable folding intermediate. Ligand binding to FBP increases the apparent folding stability of the molecule. Simultaneous detection by c.d. and fluorescence indicate that the apparent increased folding stability is derived from ligand-induced aggregation of FBP.

INTRODUCTION

The essential role of intracellular folates in effecting one-carbon transfers in critical enzyme systems for DNA synthesis is well recognized (Antony, 1992). Folate-binding protein (FBP) is a glycoinositol phospholipid-anchored membrane protein that resides in caveolae or plasmalemmal vesicles of many eukaryotic cells (Elwood et al., 1986; Luhrs et al., 1987; Bhandari et al., 1988; Lee et al., 1992). The protein functions as a folate receptor in a process known as potocytosis whereby the small molecule ligand is sequestered and taken up by the cell (Anderson et al., 1992).

FBP is found in both membrane-bound and soluble forms, and the relationship between these forms remains to be clarified. Extensive sequence homology exists between the various forms (Svendsen et al., 1984; Sadasivan and Rothenberg, 1989; Elwood, 1989), but soluble FBP generally has no glycoinositol phospholipid moiety attached to its C-terminus.

Synthetic folates are intensively used as therapeutic tools in a variety of infectious, immunologic and neoplastic diseases, as well as in transplantation and tumour biology (Antony, 1992). Because FBP would also act as a carrier of folate analogues, the structural basis for the interaction between FBP and folate is of considerable interest. Little is known about the structure of the folate-binding site or the structural consequences of ligand binding. Since soluble FBP retains high-affinity folate binding it constitutes a useful model system for the study of the interaction between folate and its receptor.

We have employed c.d. and fluorescence spectroscopy to characterize structural implications of folate binding to soluble FBP from cow's milk, a 222-residue protein that displays high-affinity ligand binding (Svendsen et al., 1979; Hansen et al., 1983). These tools provide spectroscopic signatures of FBP conformation and show that folate binding affects both the structure and folding stability of the FBP molecule.

MATERIALS AND METHODS

Materials

FBP was isolated from cow's whey and purified as described (Svendsen et al., 1979). Folate (PGA) was purchased from Sigma and guanidinium chloride (ultra pure grade) (GdmCl) was the product of Schwart/Mann Biotech. All other chemicals employed in these studies were reagent grade or better. Milli-Q (Millipore)-filtered water was used throughout.

Protein preparation

A concentrated stock solution (10 mg/ml) of FBP in 0.2 M sodium acetate buffer, pH 5.0, was stored frozen until required. Where appropriate, buffer change was accomplished by ultrafiltration using an Amicon filtration cell equipped with a PM-10 membrane (Millipore). Protein concentrations were determined by u.v. absorbance using $\epsilon_{280} = 6.816 \times 10^4\ M^{-1} \cdot cm^{-1}$. This value is based on a molecular mass of 29 kDa (Svendsen et al., 1979).

C.d. spectroscopy

C.d. spectra were recorded on a Jobin Yvon model V dichrograph calibrated with (+)-10-camphorsulphonic acid. All spectra were recorded at 25 °C. Spectra for determination of secondary structure (180–260 nm) were recorded with a cell pathlength of 0.01 cm. The protein concentration was typically about 1 mg/ml and the ionic strength kept sufficiently low so that the total absorbance of protein plus solvent was less than 1.0 at 190 nm. Denaturation samples were scanned between 218 and 250 nm using a 0.2 cm pathlength. Typical protein concentrations were 5 μM.

All spectra were smoothed with a Fourier transform algorithm and the appropriate background spectra subtracted. The result, $\Delta\epsilon$, is based on the molar concentration of peptide bond. Secondary structures were predicted from 180–260 nm c.d.

Abbreviations used: FBP, folate-binding protein; PGA, *N*-{4-[(2-amino-1,4-dihydro-4-oxopteridin-6-ylmethyl)amino]benzoyl}glutamic acid (folate); GdmCl, guanidinium chloride.

§ To whom correspondence should be addressed.

spectra using singular value decomposition combined with variable selection (Hennessey and Johnson, 1981). For this purpose, a set of 22 reference proteins with known c.d. spectra and X-ray structures was used (Johnson, 1990). The procedure eliminates up to five of the 22 reference proteins and selects a number of subsets from the remainders where the sum of secondary structures is close to 100% and a good fit between the calculated and experimental spectra is obtained. For each spectrum, the result is presented as the mean ± S.D. of secondary structures predicted by the combinations (usually 15–25) that satisfy these criteria.

Fluorescence spectroscopy

Tryptophan emission spectra were recorded with a Perkin–Elmer luminescence spectrometer model LS-50. All spectra were recorded at 25 °C. Spectra obtained for the appropriate solvent blanks were subtracted from all samples. In PGA titrations, correction for a small but significant inner-filter effect was made by parallel titrations of a tryptophan solution with the same A_{280} as the protein solution in question (Birdsall et al., 1983). Both excitation and emission slits were set at 5 nm.

RESULTS AND DISCUSSION

PGA-induced changes in secondary structure of FBP

Figure 1 shows the far-u.v. c.d. spectrum of 25 μM FBP at pH 5. The spectrum shows two negative bands with the minimum at 209 nm and a shoulder located at 220 nm. A positive band shows a maximum at 192 nm, and the crossover point is located at 199 nm. Figure 1 also shows the spectra of mixtures of 25 μM FBP and 25 μM PGA at pH 5 and 7.5. The spectra of the PGA–FBP complexes at pH 5 and 7.5 are identical within experimental error and significantly different from the unligated FBP spectrum. As a result of complex-formation, the intensity of the positive band increases and the maximum shifts to 194–195 nm. The crossover point is red-shifted by 2 nm and the relative intensities of the negative bands at 209 and 220 nm are inverted. Note that 25 μM PGA *per se* has no measurable c.d. spectrum at 0.01 cm cell pathlength.

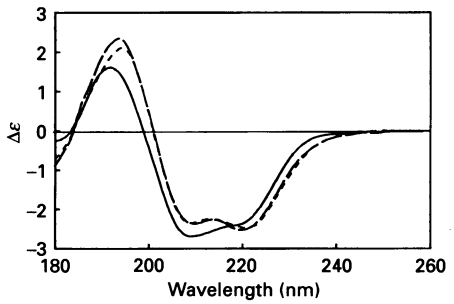

Figure 1 Far-u.v. c.d. spectra of FBP and FBP–PGA complexes in 0.01 cm cells at 25 °C

The spectrum of 25 μM unligated FBP in 10 mM sodium acetate, pH 5 (——) is compared with those of the FBP–PGA complex (25 μM FBP + 25 μM PGA) in 10 mM sodium acetate, pH 5 (— —) and 10 mM potassium phosphate, pH 7.5 (– – – –). Note that 25 μM PGA *per se* has no measurable c.d. spectrum under these conditions.

Table 1 Secondary structure contents (%) of FBP and FBP–PGA complex

	FBP pH 5	FBP–PGA pH 5	FBP–PGA pH 7.5
α-Helix	22 ± 1	24 ± 1	24 ± 1
Antiparallel β-strand	25 ± 1	15 ± 2	16 ± 1
Parallel β-strand	5 ± 1	6 ± 1	5 ± 1
Turn	17 ± 1	21 ± 1	20 ± 2
Other	31 ± 1	34 ± 1	35 ± 1
Total	100	100	100

Previous ultracentrifugation studies (Pedersen et al., 1980) have shown that the aggregation pattern of FBP is strongly dependent on pH and ligand binding. In the absence of ligand, FBP exists as a 29 kDa monomeric species at 25 μM protein, pH 5.0, whereas at pH 7–8 this concentration would lead to the formation of aggregates with an apparent molecular mass of about 300 kDa. However, owing to lack of solubility under the conditions of protein concentration and ionic strength required for c.d. spectroscopy in the far-u.v. range, it is not possible to obtain a far-u.v. c.d. spectrum of unligated FBP at pH 7.5 where aggregation occurs in the absence of ligand. In the presence of PGA, the pH profile of aggregation is qualitatively preserved, but ligand binding leads to an enhancement of aggregation. At 25 μM FBP–PGA, the average aggregation state corresponds to a mixture of monomers and dimers at pH 5, whereas at pH 7–8 aggregates with an average molecular mass of about 600 kDa are formed (Pedersen et al., 1980). Consequently, Figure 1 shows that ligand binding and/or initial aggregation (i.e. dimer formation) induces a change in secondary structure of FBP, but subsequent formation of higher aggregates does not lead to further structural change.

Table 1 summarizes the results of secondary structure analysis for free and ligated FBP. The secondary structure of FBP consists of 22% α-helix, 25% antiparallel β-strand, 5% parallel β-strand, 17% turn and 31% random coil. Previous estimates based on theoretical analysis of primary sequence data for FBP have shown an α-helix content in the range of 35–40% (Svendsen et al., 1984; Sadasivan and Rothenberg, 1989; Viswanadhan et al., 1990). The experimental data indicate that complex-formation and/or initial aggregation leads to a loss of about 10% antiparallel β-strand structure. As shown in Table 1, the loss of antiparallel β-strand is taken account of by corresponding small increases in other elements of secondary structure, notably α-helix, turn and random coil.

Effect of PGA binding on FBP tryptophan fluorescence

The tryptophan emission of FBP provides an additional spectroscopic signature of PGA binding. Figure 2(a) shows the effect of increasing amounts of PGA on the tryptophan emission spectrum of 0.18 μM FBP at pH 8. Ligand binding strongly quenches the tryptophan fluorescence with a concomitant 13 nm blue-shift of the emission maximum from 346 to 333 nm. At 346 nm, the signal is quenched 4.7-fold at saturating [PGA]. For comparison, the same additions of PGA to a 2 μM solution of tryptophan quenches only 6% of the fluorescence at 346 nm. Titrations of FBP at pH 5–7 result in a similar quench and shift in emission maximum (results not shown). At 0.18 μM protein, the ultracentrifugation data of Pedersen et al. (1980) and the gel-filtration data of Hansen et al. (1983) indicate that ligand binding enhances the aggregation of FBP at pH 7–8, whereas at pH 5 FBP is monomeric in the absence and presence of ligand. Therefore this fluorescence signal is independent of aggregation.

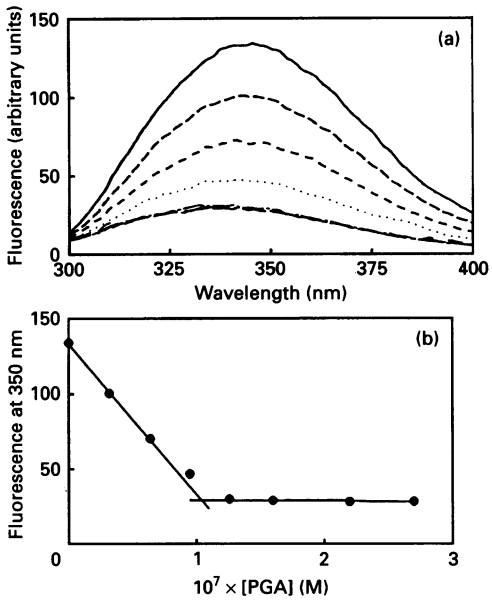

Figure 2 Tryptophan emission spectra (excitation 280 nm) of FBP and the effect of folate binding in 10 mM Tris/ClO_4^-, pH 8, at 25 °C

(**a**) Fluorescence emission spectra for 0.18 μM FBP (——) and the effect of PGA additions: 0.032 (— —), 0.064 (— — —), 0.095 (· · · ·), 0.126 (— · —), 0.160 (— · · —), 0.220 (— — —) and 0.270 (— · · —) μM. (**b**) Corrected fluorescence quench at 350 nm as a function of [PGA].

Figure 2(b) shows the extent of the quench at 350 nm as a function of [PGA] at pH 8. Since the concentrations of both PGA and FBP are orders of magnitude above K_D [approx. 1 nM (Hansen et al., 1983)], these experimental conditions result in quantitative formation of PGA–FBP at each point along the titration curve. Accordingly, the titration curve in Figure 2(b) consists of two straight lines with an intersection point corresponding to the stoichiometry of PGA binding. The observed stoichiometry of about 0.6 mol of PGA/mol of FBP is very close to that obtained from dialysis experiments using radiolabelled PGA (Hansen et al., 1983). We conclude that tryptophan is present at the PGA-binding site and/or ligand binding induces a conformation change which strongly affects tryptophan environment in FBP. We note an interesting similarity between these spectral changes and those produced by the binding of substrates and inhibitors (e.g. methotrexate) to dihydrofolate reductase (Perkins and Bertino, 1966). Hence, the quench of FBP tryptophan fluorescence provides a simple method for determination of the concentration of PGA-binding sites in a given FBP preparation. Similarly, the change in FBP tryptophan fluorescence (and corresponding changes in the ligand fluorescence) will be useful for the characterization of binding of folate analogues by FBP.

GdmCl-induced unfolding of FBP and FBP–PGA

The unfolding of FBP was monitored by both c.d. and fluorescence spectroscopy. Figure 3(a) shows c.d. spectra (218–250 nm) of monomeric FBP in the presence of increasing amounts of GdmCl. The disappearance of the negative band at 220 nm with increasing [GdmCl] indicates progressive loss of secondary structure. Dilution of samples with high [GdmCl] to

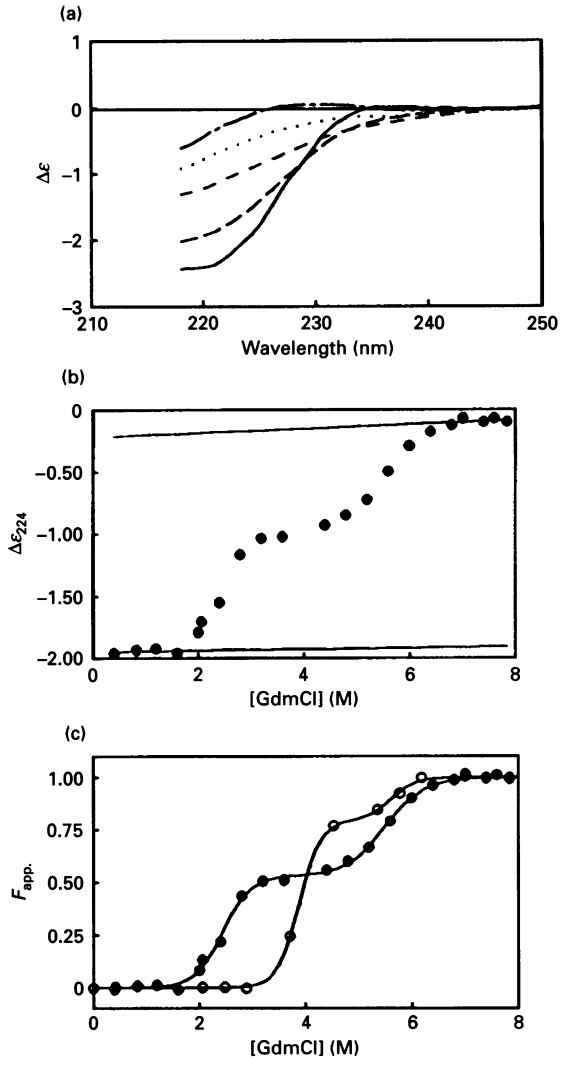

Figure 3 Unfolding of FBP and FBP–PGA detected by c.d. spectroscopy at 25 °C

(**a**) C.d. spectra of FBP as a function of [GdmCl] addition in 10 mM acetate buffer, pH 5: 0.41 (——), 2.48 (— —), 4.40 (— — —), 5.60 (· · · ·), and 6.80 (— · —) M. The protein concentration was 5 μM. (**b**) Dependence of c.d. spectra at 224 nm on [GdmCl] in 10 mM acetate, 5. The solid lines indicate the assumed dependence of c.d. of native and unfolded FBP on GdmCl concentration. (**c**) Dependence of the fractional change, $F_{app.}$, in c.d. on GdmCl concentration for 5 μM FBP at pH 5 (●) and the FBP–PGA complex (3 μM FBP + 3 μM PGA) in 10 mM potassium phosphate, pH 7.5 (○). The solid lines are calculated by using eqn. (4) and the parameters shown in Table 2.

reduce denaturant concentration resulted in recovery of the expected c.d. spectra (results not given), indicating reversible folding equilibria. As shown in Figure 3(b), $\Delta\epsilon_{224}$ depends slightly on [GdmCl] up to about 2 M. Between 2 and 6 M GdmCl, the increase in $\Delta\epsilon_{224}$ indicates that FBP undergoes a co-operative unfolding transition that results in the loss of secondary structure. Above 6–7 M GdmCl, $\Delta\epsilon_{224}$ again depends slightly on the denaturant concentration. The unfolding data of Figure 3(b) are converted into the fractional change as a function of [GdmCl]. The fractional change is defined by $F_{app.} = (\Delta\epsilon_{224} - \Delta\epsilon_{224,N})/(\Delta\epsilon_{224,U} - \Delta\epsilon_{224,N})$ where $F_{app.}$ is the apparent fractional change, $\Delta\epsilon_{224}$ is the observed value of the c.d., and $\Delta\epsilon_{224,N}$ and $\Delta\epsilon_{224,U}$ are the c.d. values for native and unfolded forms respectively at the given GdmCl concentration. Values for $\Delta\epsilon_{224,N}$ and $\Delta\epsilon_{224,U}$ at

GdmCl concentrations in the transition region are obtained by linear extrapolation of the native and unfolded baselines into the transition region. The baselines are included in Figure 3(b).

The dependence of $F_{app.}$ on GdmCl concentration is shown in Figure 3(c). The unfolding transition of FBP is clearly biphasic. The data could be fitted by a three-state model:

$$N \overset{K_{ni}}{\rightleftarrows} I \overset{K_{iu}}{\rightleftarrows} U \quad (1)$$

where the dependence of each equilibrium constant on GdmCl concentration is assumed to follow the linear denaturant binding model (Tanford, 1970):

$$K_{app.} = K_0(1+ka)^{\Delta n} \quad (2)$$

where $K_{app.}$ is the apparent equilibrium constant at a GdmCl activity a, K_0 is the equilibrium constant in the absence of GdmCl, and Δn is the difference in the number of binding sites for GdmCl between native and unfolded forms of the protein. The value of k was taken to be 0.6 (Pace, 1986). Concentrations of GdmCl were converted into activities as described by Aune and Tanford (1969). For the three-state model shown in eqn. (1), the equations become

$$K_{app.} = F_{app.}/(1-F_{app.}) = (K_{ni}K_{iu}+\alpha K_{ni})/[1+(1-\alpha)K_{ni}] \quad (3)$$

where α is the fraction of the total change in $\Delta\epsilon_{224}$ that occurs in going from N to I.

Combination of eqns. (1–3) results in eqn. (4)

$$F_{app.} = \frac{K_{0,ni}K_{0,iu}(1+ka)^{\Delta n_{ni}+\Delta n_{iu}} + \alpha K_{0,ni}(1+ka)^{\Delta n_{ni}}}{1+K_{0,ni}K_{0,iu}(1+ka)^{\Delta n_{ni}+\Delta n_{iu}} + K_{0,ni}(1+ka)^{\Delta n_{ni}}} \quad (4)$$

The fit of the unfolding data for FBP to eqn. (4) yields the parameters listed in Table 2, where $\Delta G = -RT\ln K_0$. We conclude that the denaturation transition is adequately fitted by a three-state model assuming a folding intermediate. As shown in Table 2, conversion from the native to the intermediate form contributes about one-half of the total observed c.d. change at 224 nm. Alternatively, the biphasic unfolding curve may arise from the existence of two components in the FBP preparation with widely different folding stability. We consider this possibility unlikely because FBP exists as a well-defined monomeric species under these conditions and the protein preparation meets the usual requirements for protein homogeneity (Svendsen et al., 1979).

The unfolding curve for the aggregated FBP–PGA complex is included in Figure 3(c). This transition is also biphasic; however, as shown in Table 2, the relative contribution of the two phases is shifted and ligand binding/aggregation leads to an overall enhancement of the apparent folding stability of the FBP molecule.

Table 2 Parameters for three-state fits to observed unfolding curves, namely eqn. (4)

	FBP, pH 5	FBP–PGA, pH 7.5
ΔG_{ni} (kJ/mol)	21.8	44.0
ΔG_{iu} (kJ/mol)	33.5	41.0
$\Delta G_{tot.}$ (kJ/mol)	55.3	85.0
Δn_{ni}	16.7	19.8
Δn_{iu}	17.7	12.3
α	0.50	0.77

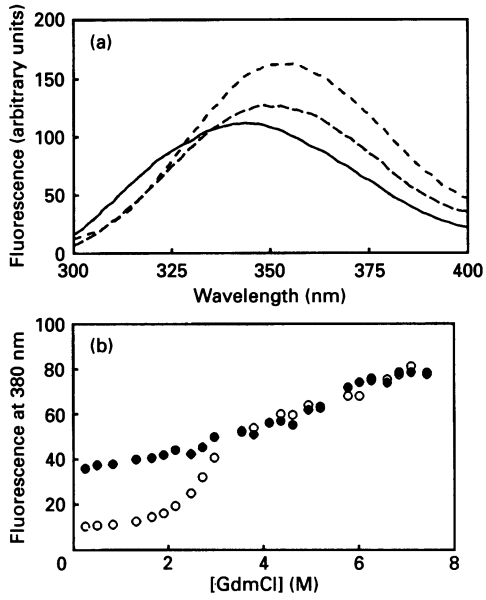

Figure 4 Fluorescence spectra (excitation 280 nm) for FBP and FBP–PGA showing the effect of increasing [GdmCl] in 10 mM Tris/ClO_4^-, pH 8, 25 °C

(**a**) Fluorescence emission spectra of 0.15 μM unligated FBP in 0.25 (——), 3.55 (— —) and 6.02 (– – – –) M GdmCl. (**b**) Fluorescence enhancement at 380 nm as a function of [GdmCl] for 0.15 μM FBP (●) and 0.15 μM FBP + 0.15 μM PGA (○).

In order to obtain additional information on the unfolding mechanism and the origins of ligand-induced stability of FBP, the unfolding transition was monitored by fluorescence. As shown in Figure 4(a), increasing concentrations of GdmCl lead to an enhancement of FBP tryptophan fluorescence. The wavelength for emission maximum increases from 346 nm to 353 nm. At 353 nm, unfolding is accompanied by a 1.5-fold fluorescence enhancement. Still, the fluorescence is only about 70% of that obtained for an equimolar tryptophan standard solution. This result indicates that part of the tryptophan residues in native FBP reside on the surface in environments that contribute to quenching. The magnitude of the fluorescence enhancement at 380 nm is plotted as a function of [GdmCl] in Figure 4(b). As unfolding proceeds, the increase in fluorescence is gradual; however, there is no sign of a co-operative transition. The non-equivalence of transitions observed by c.d. and fluorescence (compare Figures 3b and 4b) supports the hypothesis of a complex multiphasic unfolding mechanism for FBP.

Although tryptophan fluorescence is inadequate for quantitative analysis of FBP unfolding, the sensitivity to ligand binding (Figure 2) allows the determination of the point along the unfolding curve where PGA dissociation occurs. Figure 4(b) also shows the fluorescence enhancement at 380 nm for the FBP–PGA complex as a function of [GdmCl]. In contrast with the result for unligated FBP, the unfolding curve for FBP–PGA is characterized by a co-operative transition in the 2–3 M GdmCl range caused by PGA dissociation. Comparison of the c.d. and fluorescence unfolding data for FBP–PGA shows that the ligand dissociates at 2–3 M GdmCl whereas the loss of secondary

structure takes place at 3–6 M GdmCl. It follows that PGA dissociation precedes FBP unfolding in the unfolding pathway of the PGA–FBP aggregate. Hence, we conclude that the ligand-induced shift in apparent stability of FBP (Figure 3c) is primarily derived from the PGA-enhanced association of FBP.

We thank Mrs. Jytte Rasmussen for assistance in the preparation of the FBP samples used in the present investigations.

REFERENCES

Anderson, R. G. W, Kamen, B. A., Rothberg, K. G. and Lacey, S. W. (1992) Science **255**, 410–411
Antony, A. C. (1992) Blood **79**, 2807–2820
Aune, K. C. and Tanford, C. (1969) Biochemistry **8**, 4586–4590
Birdsall, B., King, R. W., Wheeler, M. R., Lewis, C. A., Groode, S. R., Dunlap, R. B. and Roberts, G. C. K. (1983) Anal. Biochem. **132**, 353–361
Bhandari, S. D., Joshi, S. K. and McMartin, K. E. (1988) Biochim. Biophys. Acta **937**, 211–218
Elwood, P. C. (1989) J. Biol. Chem. **264**, 14893–14901

Received 2 November 1992/11 January 1993; accepted 13 January 1993

Elwood, P. C., Kane, M. A., Portillo, R. M. and Kolhouse, J. F. (1986) J. Biol. Chem. **261**, 15416–15423
Hansen, S. I., Holm, J., Lyngbye, J., Pedersen, T. G. and Svendsen, I. (1983) Arch. Biochem. Biophys. **226**, 636–642
Hennessey, J. P. and Johnson, W. C. (1981) Biochemistry **20**, 1085–1094
Johnson, W. C. (1990) Proteins **7**, 205–214
Lee, H.-C., Shoda, R., Krall, J. A., Foster, J. D., Selhub, J. and Rosenberry, T. L. (1992) Biochemistry **31**, 3236–3243
Luhrs, C. A., Pitiranggon, P., Costa, M. D., Rothenberg, S. P., Slomiany, B. L., Brink, L., Tous, G. I. and Stein, S. (1987) Proc. Natl. Acad. Sci. U.S.A. **84**, 6546–6549
Pace, C. N. (1986) Methods Enzymol. **131**, 266–280
Pedersen, T. G., Svendsen, I., Hansen, S. I., Holm, J. and Lyngbye, J. (1980) Carlsberg Res. Commun. **45**, 161–166
Perkins, J. P. and Bertino, J. R. (1966) Biochemistry **5**, 1005–1012
Sadasivan, E. and Rothenberg, S. P. (1989) J. Biol. Chem. **264**, 5806–5811
Svendsen, I., Martin, B., Pedersen, T. G., Hansen, S. I., Holm, J. and Lyngbye, J. (1979) Carlsberg Res. Commun. **44**, 89–99
Svendsen, I., Hansen, S. I., Holm, J. and Lyngbye, J. (1984) Carlsberg Res. Commun. **49**, 123–131
Tanford, C. (1970) Adv. Protein Chem. **24**, 1–95
Viswanadhan, V. N., Weinstein, J. N. and Elwood, P. C. (1990) J. Biomol. Struct. Dyn. **7**, 985–1001